QCD and collider physics
Lecture II: Infrared safety, e^+e^- annihilation and Jets

ICTP Summer School on Particle Physics, June 2023

Keith Ellis

keith.ellis@durham.ac.uk

IPPP, Durham, UK

Bibliography

QCD and Collider Physics
(Cambridge Monographs on Particle Physics, Nuclear Physics and Cosmology)
by R. K. Ellis, W.J. Stirling and B.R. Webber

Towards Jetography,
Gavin P. Salam.
arXiv:0906.1833 [hep-ph],Eur.Phys.J. C67 (2010) 637-686.

Plan

- Infra-red divergences
  - ⋆ Branching processes
  - ⋆ Infra-red safe and factorizable processes
- e^+e^- annihilation
  - ⋆ Total cross section
  - ⋆ QCD corrections to the e^+e^- cross section.
  - ⋆ Shape distributions
  - ⋆ Jet fractions
- Jet algorithms
  - ⋆ Jet algorithms in e^+e^-
  - ⋆ Inclusive k_T algorithm
  - ⋆ Cambridge-Aachen algorithm
  - ⋆ Anti k_T algorithm
  - ⋆ Infra-red safety of sequential recombination algorithms

Infrared divergences

- Even in high-energy, short-distance regime, low energy aspects of QCD cannot be ignored. Soft or collinear gluon emission gives infrared divergences in PT. Light quarks ($m_q \ll \Lambda$) also lead to divergences in the limit $m_q \to 0$ (mass singularities).

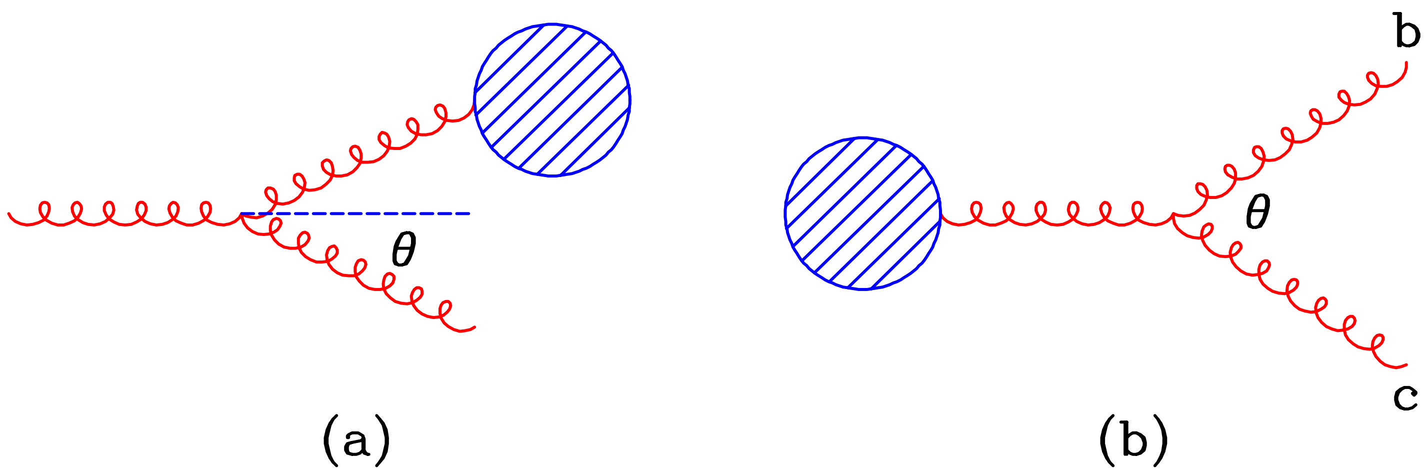

⋆ Spacelike branching: gluon splitting on incoming line (a)

$$p_b^2 = -2E_a E_c (1 - \cos\theta) \leq 0 \ .$$

Propagator factor $1/p_b^2$ diverges as $E_c \to 0$ (soft singularity) or $\theta \to 0$ (collinear or mass singularity).

If a and b are quarks, inverse propagator factor is

$$p_b^2 - m_q^2 = -2E_a E_c(1 - v_a \cos\theta) \leq 0 \ ,$$

Hence $E_c \to 0$ soft divergence remains; collinear enhancement becomes a divergence as $v_a \to 1$, i.e. when quark mass is negligible. If emitted parton c is a quark, vertex factor cancels $E_c \to 0$ divergence.

- Timelike branching: gluon splitting on outgoing line (b)

  $$p_a^2 = 2E_b E_c(1 - \cos\theta) \geq 0 \ .$$

  Diverges when either emitted gluon is soft (E_b or $E_c \to 0$) or when opening angle $\theta \to 0$. If b and/or c are quarks, collinear/mass singularity in $m_q \to 0$ limit. Again, soft quark divergences cancelled by vertex factor.

- Similar infrared divergences in loop diagrams, associated with soft and/or collinear configurations of virtual partons within region of integration of loop momenta.
- Infrared divergences indicate dependence on long-distance aspects of QCD not correctly described by PT. Divergent (or enhanced) propagators imply propagation of partons over long distances. When distance becomes comparable with hadron size ~ 1 fm, quasi-free partons of perturbative calculation are confined/hadronized non-perturbatively, and apparent divergences disappear.

Calculable quantities

- Can still use PT to perform calculations, provided we limit ourselves to two classes of observables:
  - ⋆ Infrared safe quantities, i.e. those insensitive to soft or collinear branching. Infrared divergences in PT calculation either cancel between real and virtual contributions or are removed by kinematic factors. Such quantities are determined primarily by hard, short-distance physics; long-distance effects give power corrections, suppressed by inverse powers of a large momentum scale.
  - ⋆ Factorizable quantities, i.e. those in which infrared sensitivity can be absorbed into an overall non-perturbative factor, to be determined experimentally.
- In either case, infrared divergences must be *regularized* during PT calculation, even though they cancel or factorize in the end.
  - ⋆ Gluon mass regularization: introduce finite gluon mass, set to zero at end of calculation. However, as we saw, gluon mass breaks gauge invariance.
  - ⋆ Dimensional regularization: analogous to that used for ultraviolet divergences, except we must *increase* dimension of space-time, $\epsilon = 2 - \frac{D}{2} < 0$. Divergences are replaced by powers of $1/\epsilon$.

e^+e^- *annihilation cross section*

- $e^+e^- \to \mu^+\mu^-$ is a fundamental electroweak processes.
- Same type of process, $e^+e^- \to q\bar{q}$, will produce hadrons. Cross sections are roughly proportional.

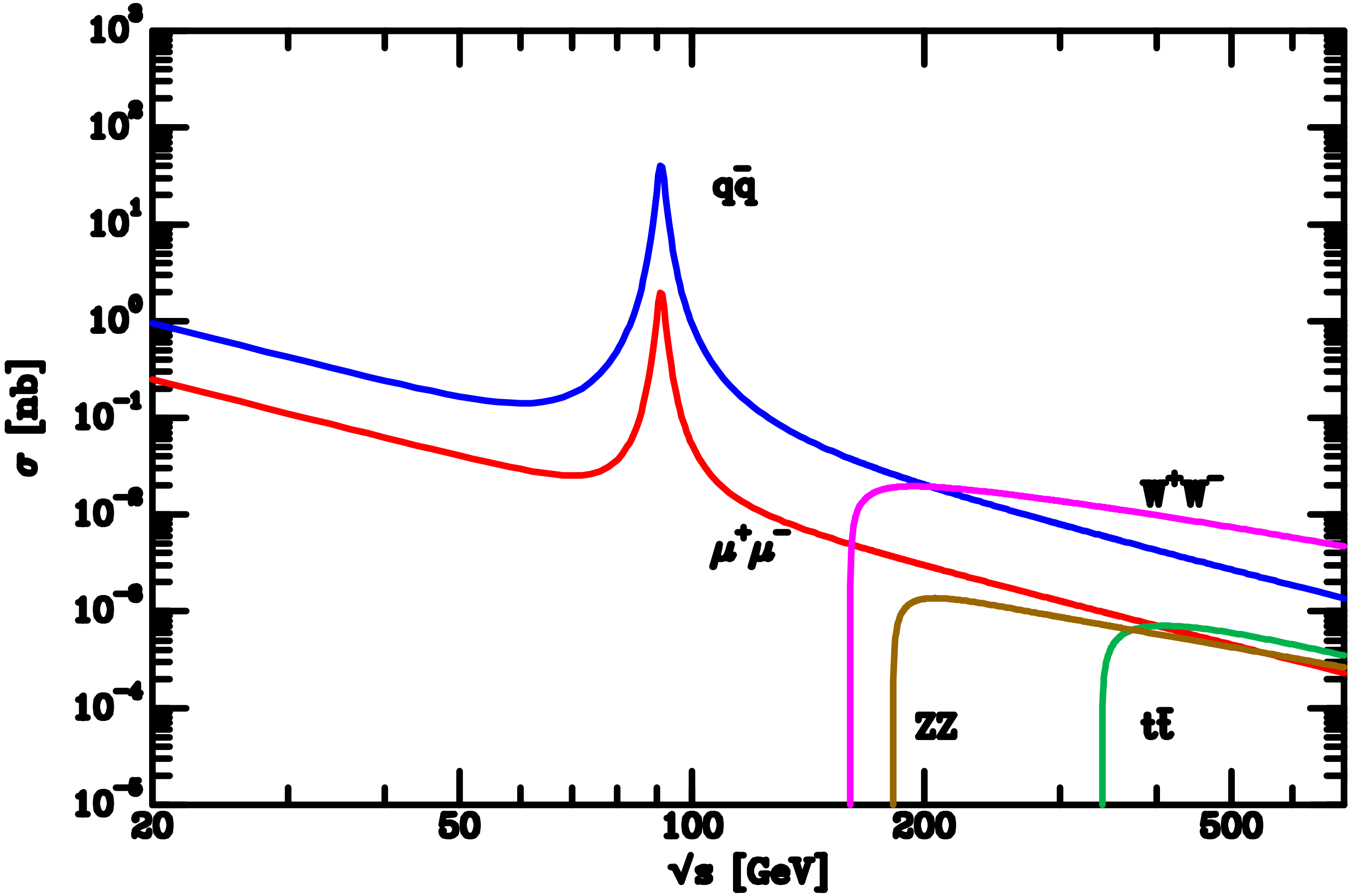

- At high energy cross sections fall like $1/s$.

Parenthetical remark

- We have reason to be interested in even smaller cross sections at an e^+e^- collider. e^+e^- measurements can give *inter alia* a model-independent measurement of the Higgs width.

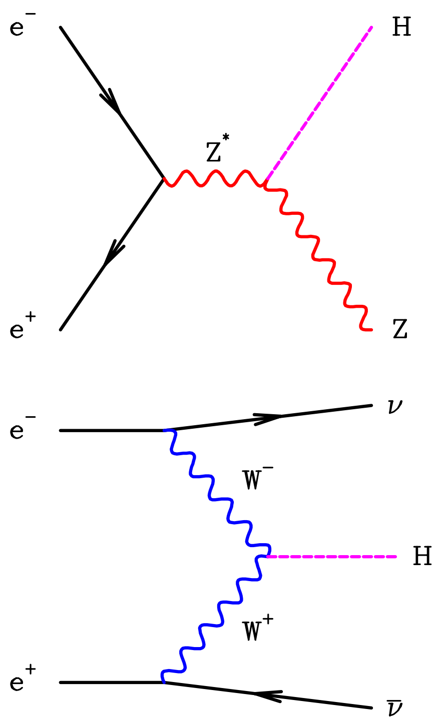

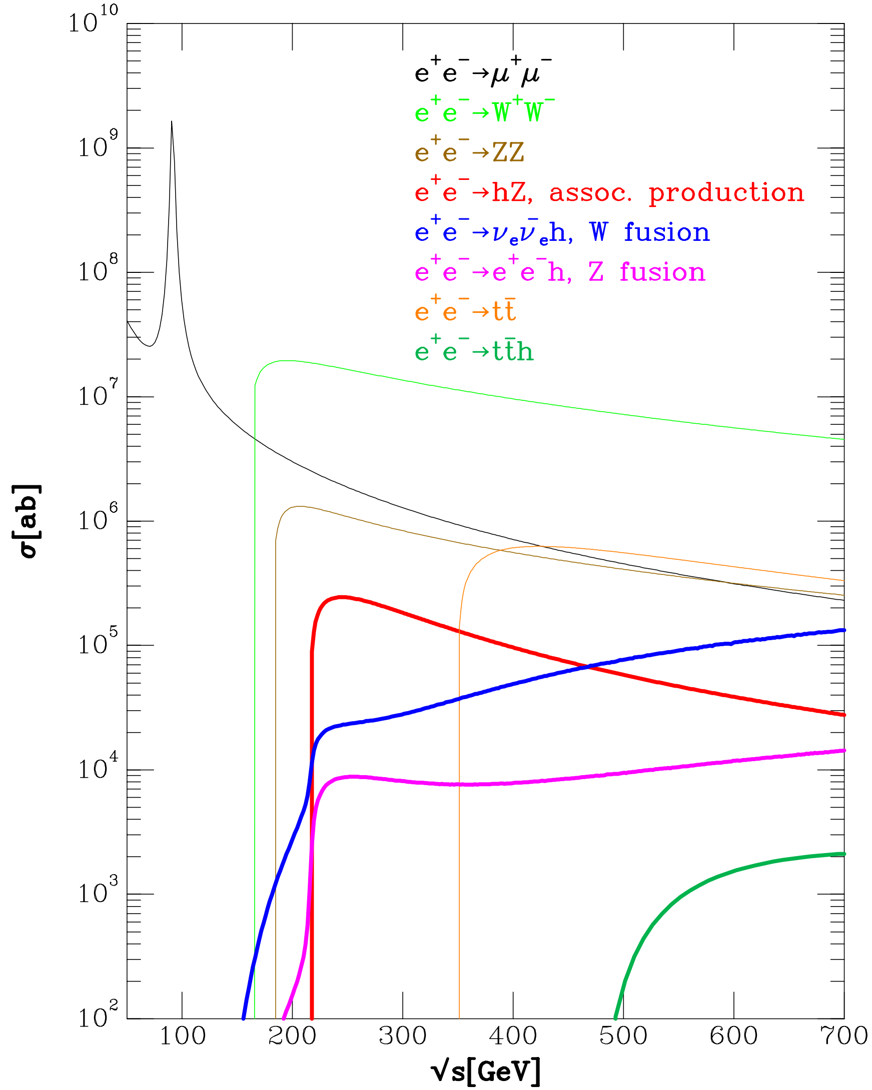

e^+e^- to hadrons

- Since formation of hadrons is non-perturbative, how can perturbation theory give hadronic cross section? This can be understood by visualizing event in space-time:
  - ⋆ e^+ and e^- collide to form γ or Z^0 with virtual mass $Q = \sqrt{s}$. This fluctuates into $q\bar{q}$, $q\bar{q}g$,..., occupy space-time volume $\sim 1/Q$. At large Q, rate for this short-distance process given by PT.

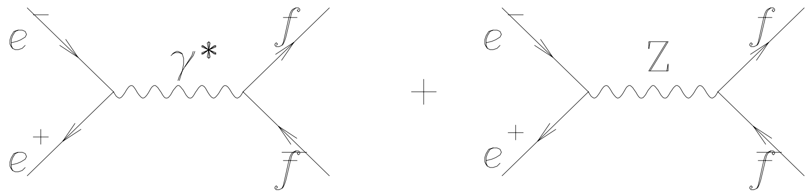

  - ⋆ Subsequently, at much later time $\sim 1/\Lambda$, produced quarks and gluons form hadrons. This modifies outgoing state, but occurs too late to change original probability for event to happen.
- Well below Z^0, process $e^+e^- \to f\bar{f}$ is purely electromagnetic, with lowest-order (Born) cross section (neglecting quark masses)

$$\sigma = N_c\,\sigma_0, \;\; \sigma_0 = \frac{4\pi\alpha^2}{3s}\; Q_f^2$$

e^+e^- to hadrons

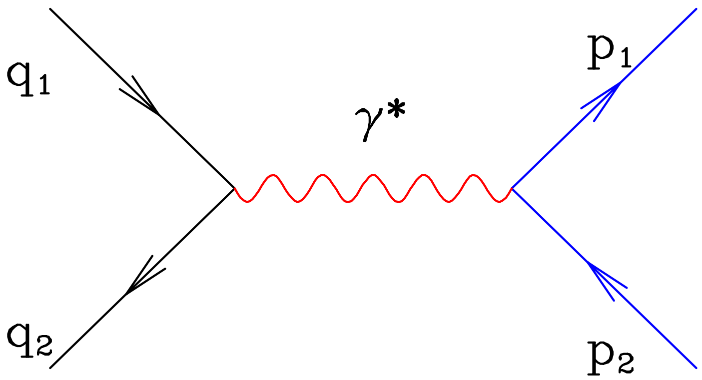

- Matrix element in Feynman gauge,

$$M = (-ie)\bar{v}(q_2)\gamma^\mu u(q_1) \times \left(\frac{-i}{(q_1+q_2)^2}\right) \times (-ie)Q_f \bar{u}(p_1)\gamma_\mu v(p_2)\,\delta_{c_1,c_2}$$

$$M = \frac{ie^2 Q_f}{(q_1+q_2)^2}\bar{v}(q_2)\gamma^\mu u(q_1)\,\delta_{c_1,c_2}\bar{u}(p_1)\gamma_\mu v(p_2)$$

$$\sum_{spins,colors}|M|^2 = \frac{e^4 Q_f^2 N_c}{((q_1+q_2)^2)^2}\sum_{spins}\;\bar{u}(q_1)\gamma^\nu v(q_2)\bar{v}(q_2)\gamma^\mu u(q_1)\times\bar{v}(p_2)\gamma_\nu u(p_1)\bar{u}(p_1)\gamma_\mu v(p$$

- using $\sum_{spins} v(q)\bar{v}(q) = \not{q}$ and $\sum_{spins} u(p)\bar{u}(p) = \not{p}$.

$$\sum_{spins,colors}|M|^2 = \frac{e^4 Q_f^2 N_c}{((q_1+q_2)^2)^2}\,\mathrm{Tr}\{\not{q}_1\gamma^\nu\not{q}_2\gamma^\mu\} \times \mathrm{Tr}\{\not{p}_2\gamma_\nu\not{p}_1\gamma_\mu\}$$

Phase space

- Two-particle massless phase space

$$PS^{(2)} = \int \frac{d^4p_1}{(2\pi)^3}\frac{d^4p_2}{(2\pi)^3}(2\pi)^4\delta^4(q_1+q_2-p_1-p_2)\,\delta(p_1^2)\,\delta(p_2^2)$$
$$= \frac{1}{16\pi}\int_{-1}^{1} d\cos(\theta)$$

- θ is the centre-of-mass scatering angle.
- Volume of n-particle massless phase space is,

$$PS^{(n)} = \frac{1}{(n-1)!\,(n-2)!}\Big(2\pi\Big)^{(4-3n)}\left(\frac{\pi}{2}\right)^{(n-1)} s^{(n-2)}$$

- For $n=2$,

$$PS^{(2)} = \left(\frac{1}{2\pi}\right)^2\left(\frac{\pi}{2}\right) = \frac{1}{8\pi}$$

Calculation of trace with Form

```
FORM 4.3.1 (Apr 11 2023, v4.3.1) 64-bits          Run: Tue Jun 13 17:24:15 20
    Off stats;
    * Declare vectors
    V q1,q2,p1,p2;
    * Declare indices
    I mu,nu,j1,j2;
    * Declare scalars
    S s,t,u,e,Qf,ave,theta,flux,PS,alpha,pi,costh,dcosth,Nc;
    .global
    * Define Strings of Gamma matrices
    G Msq=ave*e^4*Qf^2*g_(j1,q1,nu,q2,mu)*g_(j2,p2,nu,p1,mu)/s^2*Nc;
    Id,ave=1/4;
    * Take the traces;
    Trace4,j1;Trace4,j2;
    * simplify dot products
    Id,p1.q1=-t/2;Id,p2.q2=-t/2;Id,p1.q2=-u/2;Id,p2.q1=-u/2;
    Id,t=-s/2*(1-costh);Id,u=-s/2*(1+costh);
    B e,Qf,Nc;
    Print;
    .store
   Msq = + e^4*Qf^2*Nc * ( 1 + costh^2 );
    L sigma=1/flux*PS*Msq;
    Id,flux^-1=1/2/s;Id,e^2=4*pi*alpha;Id,PS=1/16/pi*dcosth;
    Id,dcosth*costh^2=2/3;Id,dcosth=2;
    Print;
    .end
   sigma = 4/3*s^-1*Qf^2*alpha^2*pi*Nc;
```

The ratio R

- Thus ($3 = N =$ number of possible $q\bar{q}$ colours)

$$R \equiv \frac{\sigma(e^+e^- \to \text{hadrons})}{\sigma(e^+e^- \to \mu^+\mu^-)} = \frac{\sum_q \sigma(e^+e^- \to q\bar{q})}{\sigma(e^+e^- \to \mu^+\mu^-)} = 3\sum_q Q_q^2 \,.$$

- On Z^0 pole, $\sqrt{s} = M_Z$, neglecting γ/Z interference

$$\sigma_0 = \frac{4\pi\alpha^2\kappa^2}{3\Gamma_Z^2}\,(a_e^2 + v_e^2)\,(a_f^2 + v_f^2)$$

where $\kappa = \sqrt{2}G_F M_Z^2/4\pi\alpha = 1/\sin^2(2\theta_W) \simeq 1.5$. Hence

$$R_Z = \frac{\Gamma(Z \to \text{hadrons})}{\Gamma(Z \to \mu^+\mu^-)} = \frac{\sum_q \Gamma(Z \to q\bar{q})}{\Gamma(Z \to \mu^+\mu^-)} = \frac{3\sum_q (a_q^2 + v_q^2)}{a_\mu^2 + v_\mu^2}$$

The couplings to the Z are specified by the $SU(2)_L \times U(1)$ structure

$$v_f = T_f^3 - 2Q_f \sin^2\theta_W\,, \quad a_f = T_f^3$$

where $T_f^3 = \frac{1}{2}$ for $f = \nu, u, \ldots$ and $T_f^3 = -\frac{1}{2}$ for $f = e, d, \ldots$.

Comparison with data

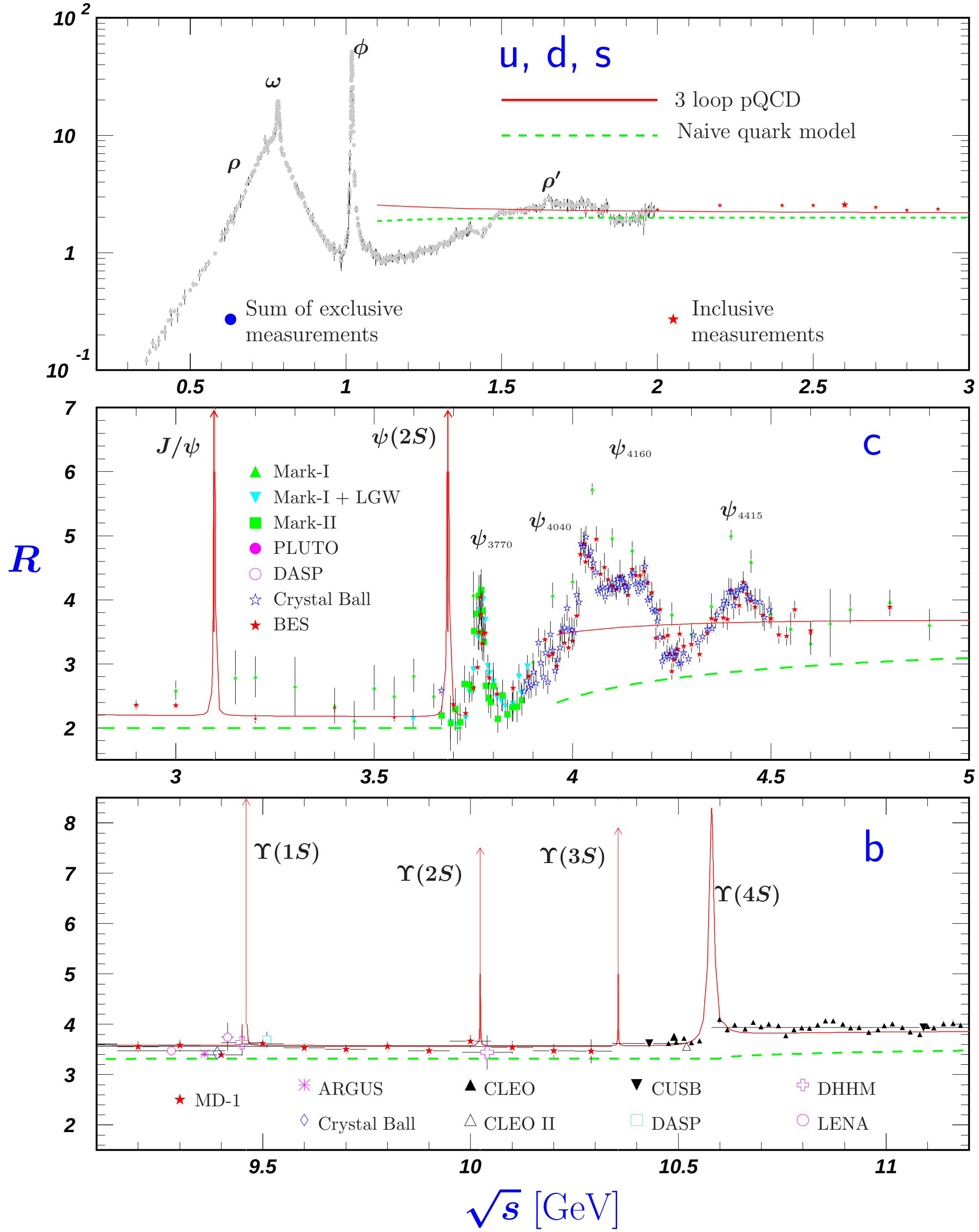

$$R = 3[(\frac{2}{3})^2 + 2(\frac{1}{3})^2] = 2$$

$$R = 3[2(\frac{2}{3})^2 + 2(\frac{1}{3})^2] = \frac{10}{3}$$

$$R = 3[2(\frac{2}{3})^2 + 3(\frac{1}{3})^2] = \frac{11}{3}$$

QCD corrections to e^+e^- to hadrons

- Measured cross section is about 5% higher than σ_0, due to QCD corrections. For massless quarks, corrections to R and R_Z are equal. To $\mathcal{O}(\alpha_S)$ we have:

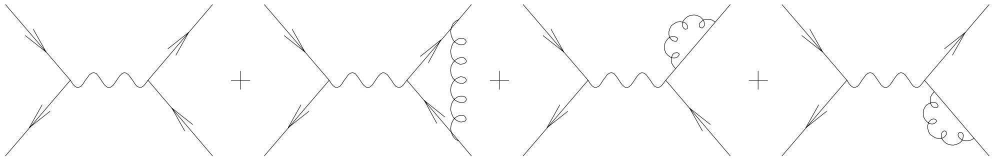

(a)

- Real emission diagrams (b):
  - ⋆ Write 3-body phase-space integration as

$$d\Phi_3 = [...] d\alpha \, d\beta \, d\gamma \, dx_1 \, dx_2 \ ,$$

α, β, γ are Euler angles of 3-parton plane,
$x_1 = 2p_1 \cdot q/q^2 = 2E_q/\sqrt{s}$,
$x_2 = 2p_2 \cdot q/q^2 = 2E_{\bar{q}}/\sqrt{s}$.

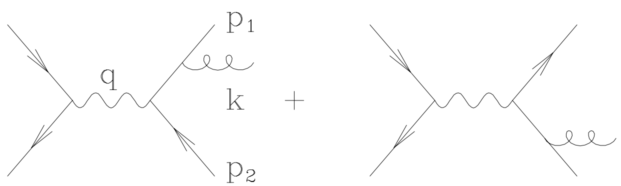

(b)

  - ⋆ Applying Feynman rules and integrating over Euler angles:

$$\sigma^{q\bar{q}g} = 3\sigma_0 C_F \frac{\alpha_S}{2\pi} \int dx_1 \, dx_2 \frac{x_1^2 + x_2^2}{(1-x_1)(1-x_2)} \ .$$

Integration of real radiation

- Integration region: $0 \leq x_1, x_2, x_3 \leq 1$ where $x_3 = 2k \cdot q/q^2 = 2E_g/\sqrt{s} = 2 - x_1 - x_2$.
- Integral divergent at $x_{1,2} = 1$:

$$\begin{aligned} 1 - x_1 &= \frac{1}{2} x_2 x_3 (1 - \cos\theta_{qg}) \\ 1 - x_2 &= \frac{1}{2} x_1 x_3 (1 - \cos\theta_{\bar{q}g}) \end{aligned}$$

- Divergences:
  - ⋆ collinear when $\theta_{qg} \to 0$ or $\theta_{\bar{q}g} \to 0$;
  - ⋆ soft when $E_g \to 0$, i.e. $x_3 \to 0$.
- If the singularities do not surivive in our observable, they are not physical – simply indicate breakdown of PT when energies and/or invariant masses approach QCD scale Λ.

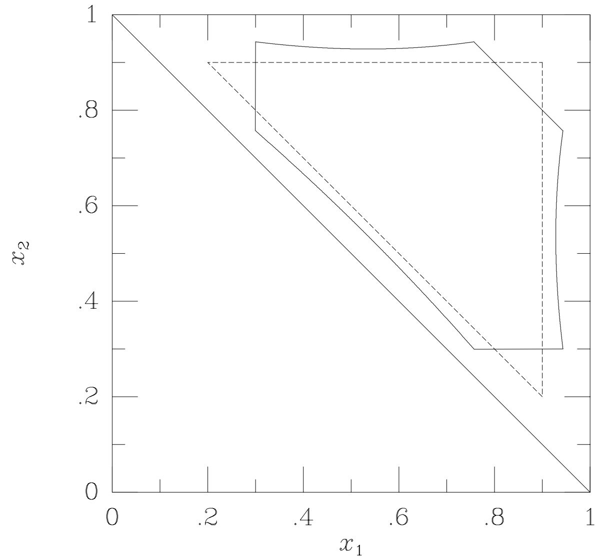

Integration with dimensional regularization

- Collinear and/or soft regions do not in fact make important contribution to R. To see this, make integrals finite using dimensional regularization, $D = 4 - 2\epsilon$ with $\epsilon < 0$. Then

$$\sigma^{q\bar{q}g} = 2\sigma_0 \frac{\alpha_S}{\pi} H(\epsilon)$$

$$\times \quad \int \frac{dx_1 dx_2}{P(x_1, x_2)} \left[\frac{(1-\epsilon)(x_1^2 + x_2^2) + 2\epsilon(1-x_3)}{[(1-x_1)(1-x_2)]} - 2\epsilon \right]$$

where $\quad H(\epsilon) = \dfrac{3(1-\epsilon)(4\pi)^{2\epsilon}}{(3-2\epsilon)\Gamma(2-2\epsilon)} = 1 + \mathcal{O}(\epsilon)$.

and $\quad P(x_1, x_2) = [(1-x_1)(1-x_2)(1-x_3)]^{\epsilon}$

- Perform the integration over x_1 by performing the transformation $x_1 = 1 - x_2(1-y)$,

$$\int_{1-x_2}^{1} dx_1 = x_2 \int_0^1 dy$$

-

$$\sigma^{q\bar{q}g} = 2\sigma_0 \frac{\alpha_S}{\pi} H(\epsilon) \left[\frac{2}{\epsilon^2} + \frac{3}{\epsilon} + \frac{19}{2} - \pi^2 + \mathcal{O}(\epsilon) \right] .$$

- Soft and collinear singularities are regulated, appearing instead as poles at $D = 4$.

Gamma Function

- In order to perform the integration we needed information about the gamma function and the beta function (of mathematics, not QCD!).
- $\Gamma(z) = \int_0^\infty \, dt \, e^{-t} t^{z-1}$
- $z\Gamma(z) = \Gamma(z+1)$
- $\Gamma(1) = 1$
- $B(a,b) = \int_0^1 dx \, x^{a-1}(1-x)^{b-1}$
- $B(a,b) = \frac{\Gamma(a)\Gamma(b)}{\Gamma(a+b)}$

Completion of total cross section

- Virtual gluon contributions (a): using dimensional regularization again

$$\sigma^{q\bar{q}} = 3\sigma_0 \left\{1 + \frac{2\alpha_S}{3\pi} H(\epsilon) \left[-\frac{2}{\epsilon^2} - \frac{3}{\epsilon} - 8 + \pi^2 + \mathcal{O}(\epsilon)\right]\right\} .$$

- Adding real and virtual contributions, poles cancel and result is finite as $\epsilon \to 0$:

$$R = 3\sum_q Q_q^2 \left\{1 + \frac{\alpha_S}{\pi} + \mathcal{O}(\alpha_S^2)\right\} .$$

  Thus R is an infrared safe quantity.

- Coupling α_S evaluated at renormalization scale μ. UV divergences in R cancel to $\mathcal{O}(\alpha_S)$, so coefficient of α_S independent of μ. At $\mathcal{O}(\alpha_S^2)$ and higher, UV divergences make coefficients renormalization scheme dependent:

$$R = 3\, K_{QCD} \sum_q Q_q^2 \; ,$$

$$K_{QCD} = 1 + \frac{\alpha_S(\mu^2)}{\pi} + \sum_{n\geq 2} C_n \left(\frac{s}{\mu^2}\right) \left(\frac{\alpha_S(\mu^2)}{\pi}\right)^n$$

Higher order coefficients

- $R = K_{QCD}\, 3 \sum_f Q_f^2$
- $K_{QCD} = 1 + \frac{\alpha_s(\mu^2)}{\pi} + \sum_{n\geq 2} C_n\left(\frac{s}{\mu^2}\right)\left(\frac{\alpha_s(\mu^2)}{\pi}\right)^n$
- In $\overline{\text{MS}}$ scheme with scale $\mu = \sqrt{s}$,

$$\begin{aligned} C_2(1) &= \frac{365}{24} - 11\zeta(3) - [11 - 8\zeta(3)]\frac{N_f}{12}, \quad \zeta(3) = 1.2020569\ldots \\ &\simeq 1.986 - 0.115 N_f \end{aligned}$$

- Coefficient C_3 is also known.
- Scale dependence of $C_2,\ C_3\ \ldots$ fixed by requirement that, order-by-order, series should be independent of μ. For example

$$C_2\left(\frac{s}{\mu^2}\right) = C_2(1) - \frac{\beta_0}{4}\log\frac{s}{\mu^2}$$

where $\beta_0 = 4\pi b = 11 - 2N_f/3$.

Scheme and scale dependence

- Scale and scheme dependence only cancels completely when series is computed to all orders. Scale change at $\mathcal{O}(\alpha_S^n)$ induces changes at $\mathcal{O}(\alpha_S^{n+1})$. The more terms are added, the more stable is prediction with respect to changes in μ.

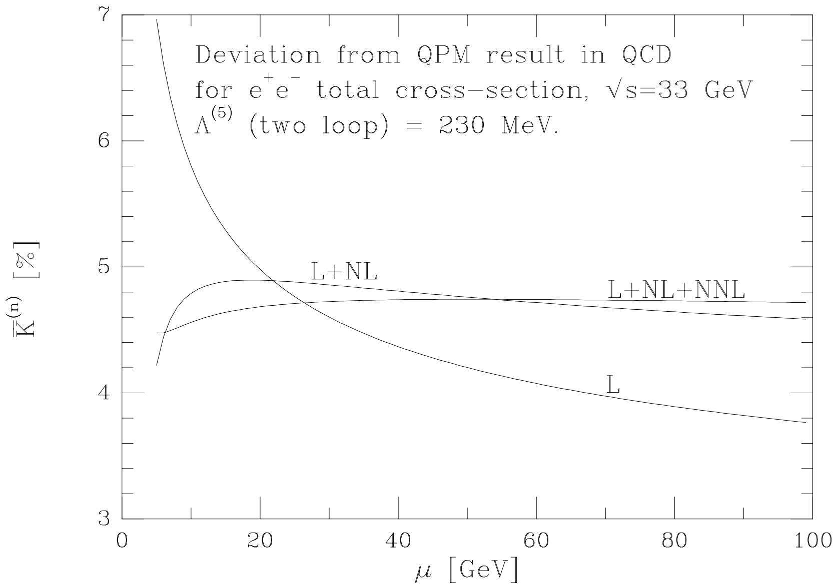

- Residual scale dependence is an important source of uncertainty in QCD predictions. One can vary scale over some 'physically reasonable' range, e.g. $\sqrt{s}/2 < \mu < 2\sqrt{s}$, to try to quantify this uncertainty. But there is no real substitute for a full higher-order calculation.

Shape distributions

- Shape variables measure some aspect of shape of hadronic final state, e.g. whether it is pencil-like, planar, spherical etc.
- For $d\sigma/dX$ to be calculable in PT, shape variable X should be infrared safe, i.e. insensitive to emission of soft or collinear particles. In particular, X must be invariant under $\boldsymbol{p}_i \to \boldsymbol{p}_j + \boldsymbol{p}_k$ whenever $\boldsymbol{p}_j$ and $\boldsymbol{p}_k$ are parallel or one of them goes to zero.
- Examples are Thrust and C-parameter:

$$T = \max \frac{\sum_i |\boldsymbol{p}_i \cdot \boldsymbol{n}|}{\sum_i |\boldsymbol{p}_i|}$$

$$C = \frac{3}{2} \frac{\sum_{i,j} |\boldsymbol{p}_i|\,|\boldsymbol{p}_j| \sin^2\theta_{ij}}{(\sum_i |\boldsymbol{p}_i|)^2}$$

After maximization, unit vector $\boldsymbol{n}$ defines *thrust axis*.

- In Born approximation final state is $q\bar{q}$ and $1 - T = C = 0$. Non-zero contribution at $\mathcal{O}(\alpha_S)$ comes from $e^+e^- \to q\bar{q}g$. Recall distribution of $x_i = 2E_i/\sqrt{s}$:

$$\frac{1}{\sigma}\frac{d^2\sigma}{dx_1 dx_2} = C_F \frac{\alpha_S}{2\pi} \frac{x_1^2 + x_2^2}{(1-x_1)(1-x_2)} .$$

Distribution of shape variable X is obtained by integrating over x_1 and x_2 with constraint $\delta(X - f_X(x_1, x_2, x_3 = 2 - x_1 - x_2))$, i.e. along contour of constant X in (x_1, x_2)-plane.

- For thrust, $f_T = \max\{x_1, x_2, x_3\}$ and we find

$$\frac{1}{\sigma}\frac{d\sigma}{dT} = C_F \frac{\alpha_S}{2\pi}\left[\frac{2(3T^2 - 3T + 2)}{T(1-T)} \log\left(\frac{2T-1}{1-T}\right) - \frac{3(3T-2)(2-T)}{(1-T)}\right].$$

  This diverges as $T \to 1$, due to soft and collinear gluon singularities. Virtual gluon contribution is negative and proportional to $\delta(1-T)$, such that correct total cross section is obtained after integrating over $\frac{2}{3} \leq T \leq 1$, the physical region for two- and three-parton final states.

- $\mathcal{O}(\alpha_S^2)$ corrections also known. Comparisons with data provide test of QCD matrix elements, through shape of distribution, and measurement of α_S, from overall rate. Care must be taken near $T = 1$ where (a) hadronization effects become large, and (b) large higher-order terms of the form $\alpha_S^n \log^{2n-1}(1-T)/(1-T)$ appear in $\mathcal{O}(\alpha_S^n)$.

Delphi data

- Figure shows thrust distribution measured at LEP1 (DELPHI data) compared with theory for vector gluon (solid) or scalar gluon (dashed).

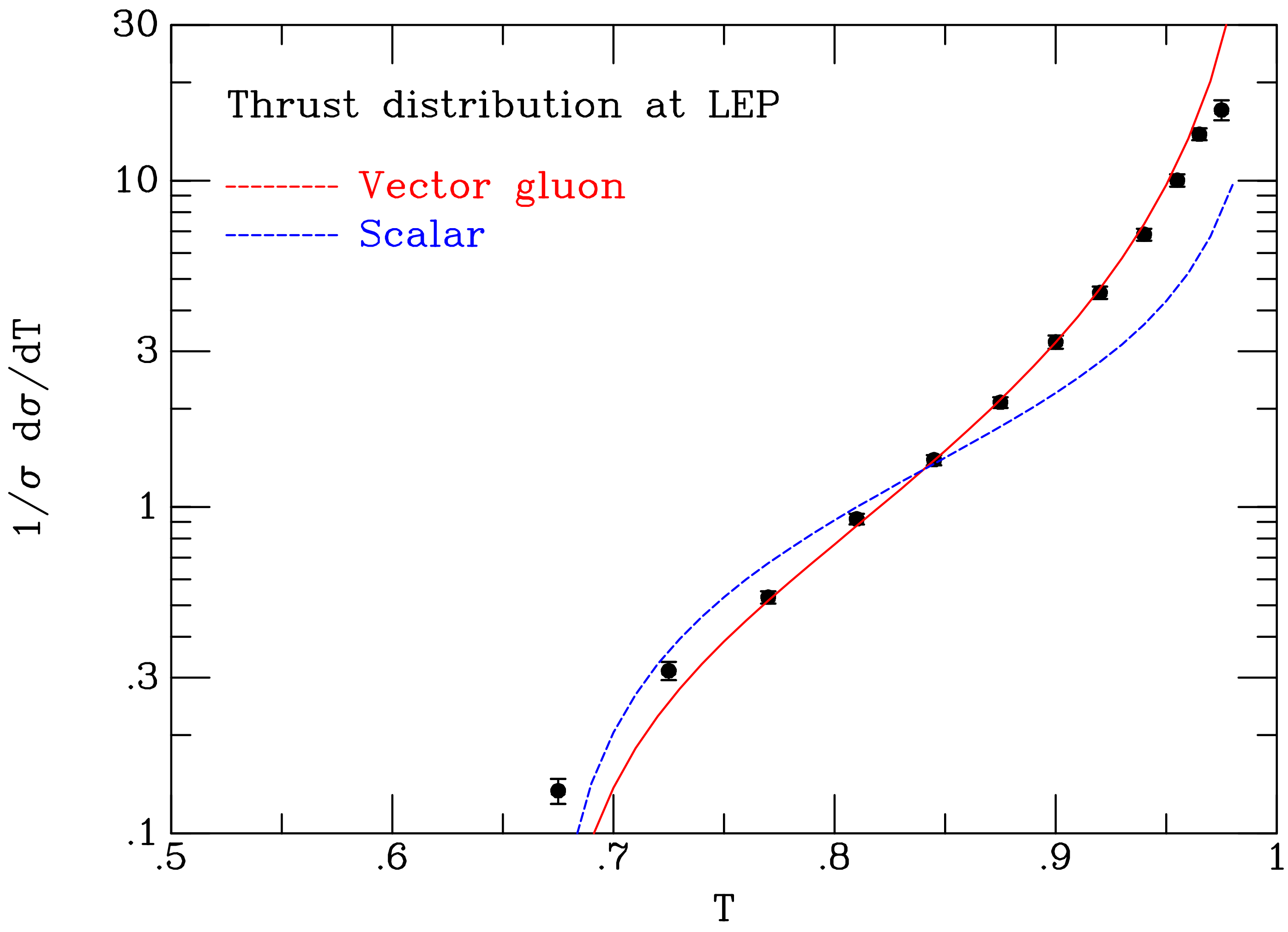

Problems with seeded cone algorithms

- Iterative cone algorithm
  - ⋆ sort all particles according to their transverse momentum
  - ⋆ Identify the particle with the largest transverse momentum as the seed particle.
  - ⋆ Draw a cone of radius ΔR about the seed particle, and identify the direction of the particles contained in the cone.
  - ⋆ If that direction does not correspond to the seed direction, adopt that direction as the new seed.
  - ⋆ When cone direction and seed direction coincide, remove particles from the eventt and iterate.
- Unfortunately the particle with the largest transverse momentum is not an collinear safe concept.

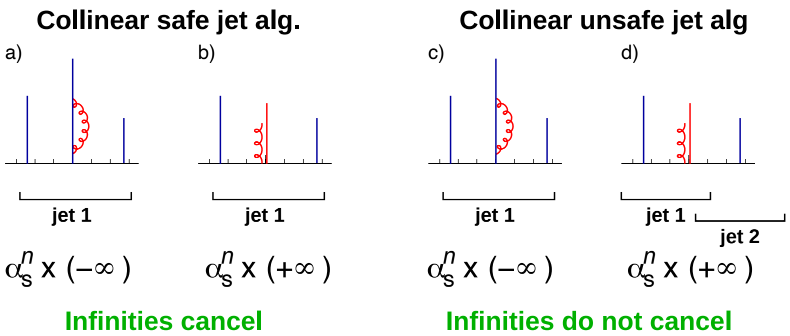

- in figure horizontal distance shows rapidity, vertical distance shows p_T

Jet algorithms

- At a hadron collider jets are clearly visible by eye.
- There are many possible mathematical procedures for defining a jet. A jet algorithm has to specify
  - ⋆ Which particles/partons are grouped together in a jet.
  - ⋆ How the momenta of the chosen particles are combined to form a pseudo-particle
- A proper jet algorithm should be insensitve to the emission of soft and collinear radiation
  - ⋆ From a theoretical point of view, this is a requirement for a finite result, which will be calculable in QCD perturbation theory
  - ⋆ From a experimental point of view, the detector will not be able to resolve collinear and/or soft hadrons.

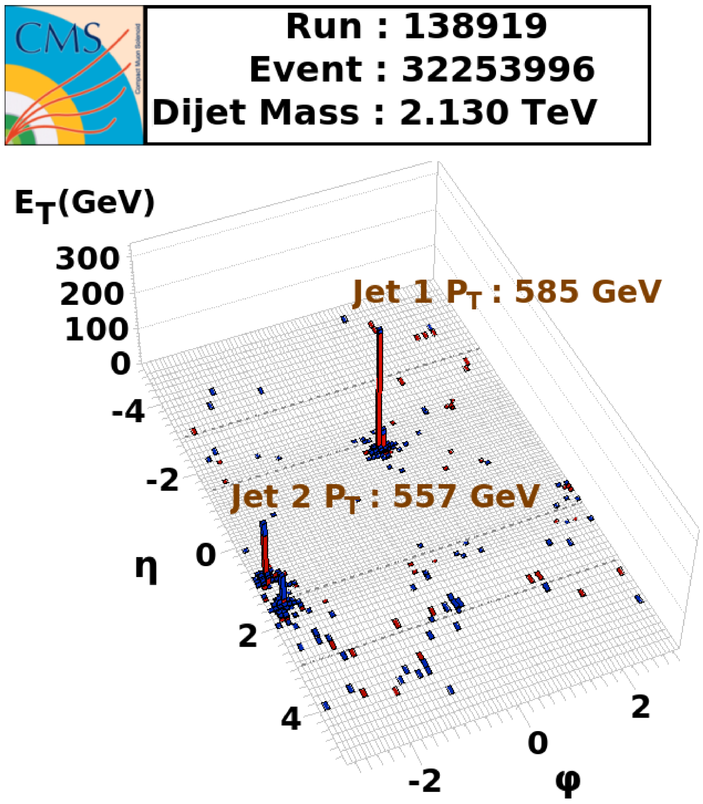

- "Lego" plot in terms of azimuthal angle and rapidity $y = \frac{1}{2}\ln(\frac{E+p_z}{E-p_z})$. For a massless particle y is identical to the pseudorapidity, $\eta = -\ln\tan(\theta/2)$.
- Rapidity is additive under longitudinal boosts.

Jet fractions

- To define fraction f_n of n-jet final states ($n = 2, 3, \ldots$), must specify jet algorithm.
- Development of a jet a series of sequential branchings. Majority of QCD branching is soft and/or collinear, with following divergences:

$$[dk_j]\, |M_{g\to g_i g_j}|^2 = \frac{2\alpha_s C_A}{\pi} \frac{dE_i}{E_i E_j} \frac{d\theta_{ij}}{\theta_{ij}} \quad E_j \ll E_i, \theta_{ij} \ll 1$$

- To invert branching process, take pair which are closest in a metric defined by the divergence structure of the theory

- This is the philosophy of k_T or Durham algorithm:
  - ⋆ Define jet resolution y_{cut} (dimensionless).
  - ⋆ For each pair of final-state momenta p_i, p_j define

$$y_{ij} = 2 \min\{E_i^2, E_j^2\}(1 - \cos\theta_{ij})/s$$

  - ⋆ If $y_{IJ} = \min\{y_{ij}\} < y_{\text{cut}}$, combine I, J into one object K with $p_K = p_I + p_J$.
  - ⋆ Repeat until $y_{IJ} > y_{\text{cut}}$. Then remaining objects are jets.

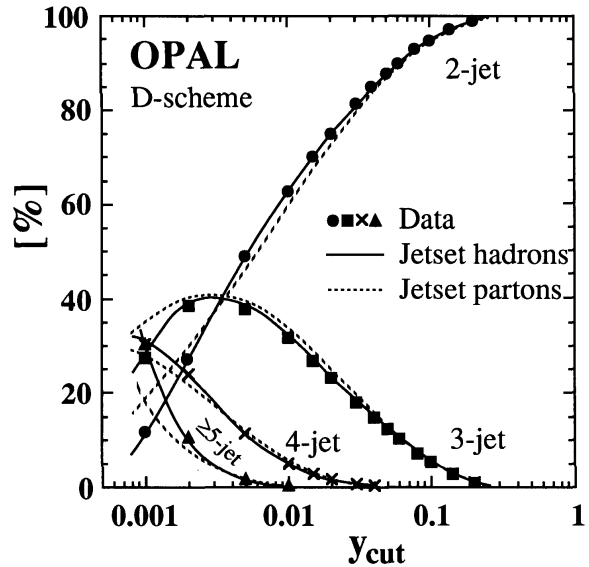

Sequential recombination jet algorithms

- Development of a jet a series of sequential branchings. Majority of QCD branching is soft and/or collinear, with following divergences:

$$[dk_j]\,|M_{g\to g_i g_j}|^2 = \frac{2\alpha_s C_A}{\pi}\frac{dE_i}{E_i E_j}\frac{d\theta_{ij}}{\theta_{ij}} \quad E_j \ll E_i, \theta_{ij} \ll 1$$

- To invert branching process, take pair which are closest in a metric defined by the divergence structure of the theory
- Definition of the k_T/Durham algorithm for hadron collisions.
  1. Calculate (or update) distances between all (pseudo-)particles i and j, (related to the relative k_T between the particles)

$$y_{ij} = 2\min(E_i^2, E_j^2)(1-\cos\theta_{ij})$$

  2. Find smallest of y_{ij}

  ⋆ If $y > y_{cut}$ stop clustering

  ⋆ else recombine i and j and repeat from step 1

Inclusive k_T algorithm

- The inclusive k_T algorithm for hadron-hadron collisions is a generalization of the e^+e^- variant.
- It belongs to the class of sequential recombination jet algorithms, which define both a jet and a clustering history.
- Introduces the new concept of a particle beam distance and the angular radius R

$$
\begin{aligned}
d_{ij} &= min(k_{Ti}^2, k_{Tj}^2)\frac{\Delta R_{ij}^2}{R^2}, \quad \Delta R_{ij}^2 = (y_i - y_j)^2 + (\phi_i - \phi_j)^2 \\
d_{iB} &= k_{Ti}^2
\end{aligned}
$$

1. Find smallest of d_{ij} , d_{iB}
2. if it is ij , combine $i + j$ and return to step 1
3. if it is iB, call i a jet, remove it from list of particles, and return to step 1
4. stop when no particles are left.

- S.D. Ellis and Soper, (hep-ph/9305266);
- Jets all separated by at least R on the lego plot.
- NB: number of jets not IR safe (soft jets near beam); number of jets above p_t cut is IR safe.
- depends on two parameters, R and p_T^{cut}

Cambridge-Aachen for hadronic collisions

- We can classify the a family sequential recombination algorithms as follows

$$
\begin{aligned}
d_{ij} &= min(k_{Ti}^{2p}, k_{Tj}^{2p}) \frac{\Delta R_{ij}^2}{R^2} \\
d_{iB} &= k_{Ti}^{2p}
\end{aligned}
$$

- The Cambridge-Aachen is the simplest jet algorithm and corresponds to $p = 0$, Wobisch and Wengler, hep-ph/990728
- Recombine the pair of objects closest in R_{ij}
- Repeat until all $R_{ij} > R$.
- The remaining objects are jets.
- Because of clustering hierachy in angle, C/A has been shown to provide the best performance when it comes to resolving jet substructure
  - ⋆ undoing the pair-wise clustering of a jet step-by-step yields its subjets
  - ⋆ Promising strategies to find e.g. high-pT top quarks and Higgs bosons are based on subjets using the C/A algorithm
- Leads to ragged edge jets

Anti-k_t

Formulated similarly to k_t (Cacciari, Salam & Soyez 0802.1189), but with

$$dij = min(1/k_{Ti}^2, 1/k_{Tj}^2)\frac{\Delta R_{ij}^2}{R^2}$$

- Anti-kt privileges the collinear divergence of QCD, favours clusterings that involve hard particles, and disfavours clustering between pairs of soft particles.
- Most pairwise clusterings involve at least one hard particle
- The algorithm involves two parameters, R the angular reach for the jets, and p_T threshold for the final jets to be taken into account.
- However since the algorithm still involves a combination of energy and angle in its distance measure, this is a collinear-safe growth, (a collinear branching gets clustered first).
- Anti-k_t leads to circular jets, which are experimentally favoured for acceptance corrections.
- Clustering sequence is not usefully related to QCD branching.

Sequential recombination algorithms:IRC safety

$$d_{ij} = \min(k_{Ti}^{2p}, k_{Tj}^{2p})\frac{\Delta R_{ij}^2}{R^2}. \quad d_{iB} = k_{Ti}^{2p}, \quad \Delta R_{ij}^2 = (y_i - y_j)^2 + (\phi_i - \phi_j)^2$$

- $p > 0$
  - New soft particle ($k_T \to 0$) means that $d \to 0 \to$ clustered first, no effect on jets
  - New collinear particle ($\Delta y^2 + \Delta\phi^2 \to 0$) means that $d \to 0 \to$ clustered first, no effect on jets
- $p = 0$
  - New soft particle ($k_T \to 0$) can be new jet of zero momentum $\to$ no effect on hard jets
  - New collinear particle ($\Delta y^2 + \Delta\phi^2 \to 0$) means that $d \to 0 \to$ clustered first, no effect on jets
- $p < 0$
  - New soft particle ($k_T \to 0$) means $d \to \infty \to$ clustered last or new zero-jet, no effect on hard jets;
  - New collinear particle ($\Delta y^2 + \Delta\phi^2 \to 0$) means that $d \to 0 \to$ clustered first, no effect on jets.

Comparison of jet algorithms,arXiv:0802.1189

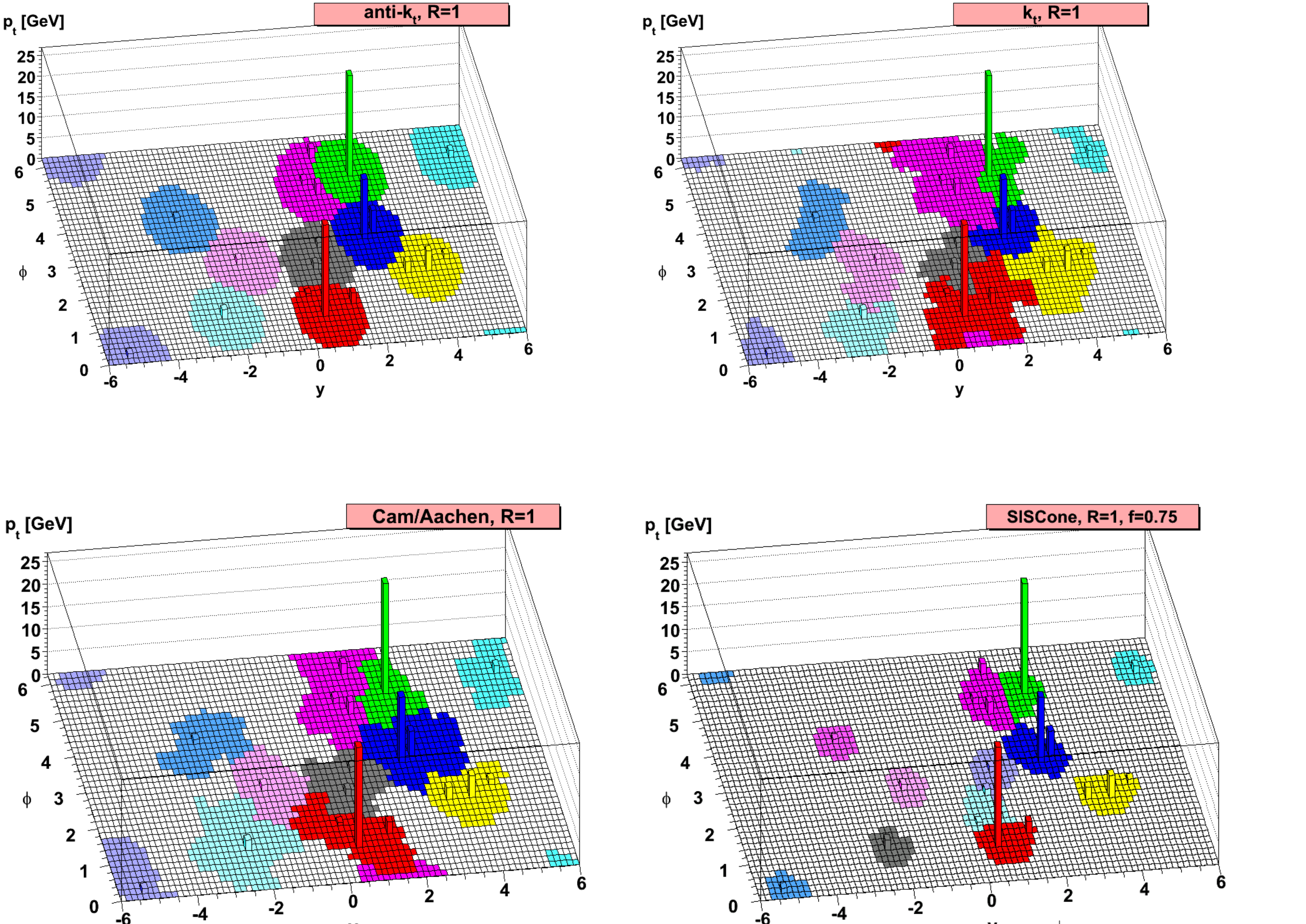

Recap

- Perturbative QCD has infrared singularities due to collinear or soft parton emission. We can calculate infra-red safe or factorizable quantities in perturbation theory because of the property of asymptotic freedom.
- Total e^+e^- cross section is an example of an infra-red finite quantity.
- IR singularities are normally regularized by dimensional regularization.
- Higher order corrections can be calculated for IR safe or factorizable quantities; because α_S is not so small, they are necessary to find agreement with the data.
- Jets are specified by a jet algorithm, depending on one or two parameters. Different algorithms (and parameters) will best capture different features of the data.
- Anti-k_T algorithm is the de facto standard at the LHC; yields all the benefits of a cone algorithm without their defects.